Experimental analysis of the scattering light for the wavelength of 532 nm through water cloud by the Monte Carlo-Mie method

E. E. Perez Mayesffer Azcarraga

Facultad de Ciencias de la Electrónica, Benemérita Universidad Autónoma de Puebla, Avenida San Claudio y 18 Sur, Colonia San Manuel, Puebla 72570.

R. Cuevas Terrones

Depto. de Electrónica, Instituto Nacional de Astrofísica, Óptica y Electrónica, Calle Luis Enrique Erro No. 1, Puebla 72840, México.

I. Zaldivar Huerta

Depto. de Electrónica, Instituto Nacional de Astrofísica, Óptica y Electrónica, Calle Luis Enrique Erro No. 1, Puebla 72840, México.

J. D. Hernández de la Luz

Centro de Investigación en Dispositivos Semiconductores CIDS-ICUAP, Benemérita Universidad Autónoma de Puebla, Avenida San Claudio y 18 Sur, Colonia San Manuel, Puebla 72570

Received 3 November 2023; accepted 24 August 2024

This paper describes an experimental analysis of the scattering of light through a cloud water. For this goal, an experimental setup to emulate a cloud of water is assembled. This arrangement is composed of an optical source emitting at the wavelength of 532 nm that is driven by a switching interface, a turbid medium, a photodiode, and an optical power meter. The optical source is modulated at the frequency of 1 Hz under Pulse Width Modulation (PWM) format. The modulated beam light travels the turbid medium, recovered by the photodiode that is connected to the power meter. The measured power data are analyzed using a novel Monte Carlo-Mie model to obtain the weighted extinction coefficient ratio probability. Subsequently, by the investment model some physical properties of the turbid medium as the refractive index and water droplet average sizes are obtained.

Keywords: Monte Carlo Method; mie scattering; turbid media; investment model.

DOI: https://doi.org/10.31349/RevMexFis.71.011302

1. Introduction

Today, people all over the world are living with a series of consequences due to additional global warming every day. It is essential to a drastic reduction of carbon dioxide and chemical aerosols and, at the same time, increment clean energy as Eolic parks and solar cells. Due to there is a risk of reaching a high value of warming to damage all living beings with the danger of a point of no return, it is very important to sensitize people and governments. In this regard, the most recent International Panel on Climate Change (IPCC) reports unprecedented menace. Also, it reports several important activities carried out by researchers focused on solving this situation. One important idea is about to reduce the impacts of solar radiation to keep global warming below 1.5 or even 2°C. In other words, the main idea is to reduce the impacts of solar radiation modification (SRM), producing reflecting incoming solar radiation by introducing a thin aerosol layer in the higher atmosphere or by brightening clouds [1]. Researchers all over the world work hard to develop new climatic models. One power model to describe aerosol profile random climatic processes is the Monte Carlo Method. The Monte Carlo Method is a broad class of computational algorithms, which rely on repeated random sampling. This method is used in some physical and mathematical problems and is most useful when it is difficult or impossible to use other mathematical methods [2]. As it is mentioned some researchers as Zhensen Wu *et al.* [3], Bissonnete L.R *et al.* [4], Toublanc Dominique *et al.* [5], Judith R. Mourant *et al.* [6], Liaparinos P.F. [7], Yuzaho Ma et al [8], Torres Garcia Eugenio *et al.* [9], Pielsticker Lucas *et al.* [10]. They propose a simplified phase function called the Henyey Greenstein function or Rutherford distribution function to describe scattering light from spherical particles, this is a traditional technique that uses director cosine to find photon paths generating very large machine cycles. This work uses a novel unity vector (uv), instead of the Mie-phase function, this uv includes a complex transversal plane that reduces the calculus of photon paths into turbid media. Besides this methodology proposes includes refractive index and average size of scatterers of the turbid media [11]. In this paper, a modified Monte Carlo- Mie (MC-M) method is used to solve scattering light as spherical harmonics from Mie theory. Applied through turbid media, generated in Laboratory. And finally, is obtained the refractive index from turbid media and average sizes from scatterer profiles. The selection of the wavelength around 520 nm is

due to its demonstrated good performance in turbid media [12-14]. The rest of this paper is organized as follows: Section 2 describes the Monte Carlo-Mie model. The experimental prototype used to corroborate the proposed modified Monte Carlo-Mie method is explained in Sec. 3. Experimental parameters and specifications are shown in Sec. 4. Simulation and results are explained in Sec. 5 and, finally, the overall conclusions are presented in Sec. 6.

2. Monte Carlo-Mie model

Monte Carlo-Mie (MC-M) model is a numerical method that uses a modified 3D unitary spatial vector (uv). The main characteristic of this unitary spatial vector is its structure, which is composed by Hanckel-Legendre-Bessel special functions and is used as a step function projected in spherical harmonics in a turbid medium. This vector is formed by a transverse plane vector that describes one spatial harmonic wave in scattering, and it is used in the Monte Carlo algorithm. The Monte Carlo method uses a probabilistic function. In particular, in this paper, the distribution function used is an exponential function, thus, the mathematical expectation is expressed as [15]

$$\mathbf{M}\lambda = \int_0^\infty x\mathbf{p}(x)dx = \int_0^\infty x\sigma\mathbf{e}^{-\sigma x}dx_{\varphi}^{'}. \tag{1}$$

Integrating by parts, the Free Advance Average Flux (λ) is determined

$$\lambda = -\frac{1}{\sigma}\ln(\gamma). \tag{2}$$

The MC-M algorithm delivers three probabilistic cases: (1) Forward photons weight ratio, (2) Back forward photon weight ratio, and (3) Trapped photons weight ratio. These cases can be present in relation with turbid media.

The following equation shows the spatial unitary vector representing one point over spatial spherical harmonics [11].

$$\hat{\nu} = (r + \lambda\mu_{k1})\hat{e}_r + (\theta + \lambda\mu_{k2})\hat{e}_\theta + (\varphi + \lambda\mu_{k3})\hat{e}_\varphi, \tag{3}$$

with scalar special functions:

$$\mu_{k1} = P_n^1(\cos k), \tag{4}$$

$$\mu_{k2} = \frac{\cos\phi}{\rho}[i\tau_n\xi_n^{'} - \pi_n\xi_n], \tag{5}$$

$$\mu_{k3} = \frac{\sin\phi}{\rho}[i\tau_n\xi_n^{'} - \pi_n\xi_n]. \tag{6}$$

Mie theory describes three parameters in scattering light theory which are extinction coefficient, scattering coefficient and absorption coefficient. These parameters are supported by the optical theorem [16]. The following equations describe their normalized forms:

$$Q_{\text{ext}} = \frac{\sigma_{\text{ext}}}{\sigma_{\text{geom}}} = \frac{2}{(ka)^2}\sum_{n=1}^{\infty}(2n+1)\mathbf{Re}(a_n + b_n), \tag{7}$$

$$Q_{\text{scatt}} = \frac{\sigma_{\text{ext}}}{\sigma_{\text{geom}}} = \frac{2}{(ka)^2}\sum_{n=1}^{\infty}(2n+1)(\mid a_n \mid^2 + \mid b_n \mid^2), \tag{8}$$

and

$$Q_{\text{abs}} = \frac{\sigma_{\text{ext}}}{\sigma_{\text{geom}}} = Q_{\text{ext}} - Q_{\text{scatt}}. \tag{9}$$

The Ricatti-Bessel (RB) functions [11,16] are used in Eq. (7) and (8) to describe the amplitude scattering wave. The Mie coefficients, from RB functions, are described in the following equations:

$$a_n = \frac{m\psi_n(mx)\psi_n^{'}(x) - \psi_n(x)\psi_n^{'}(mx)}{m\psi_n(mx)\xi_n^{'}(x) - \xi_n(x)\psi_n^{'}(mx)}, \tag{10}$$

$$b_n = \frac{\psi_n(mx)\psi_n^{'}(x) - m\psi_n(x)\psi_n^{'}(mx)}{\psi_n(mx)\xi_n^{'}(x) - m\xi_n(x)\psi_n^{'}(mx)}. \tag{11}$$

Mie theory Eqs. (1)-(9) are used in the Monte Carlo algorithm to obtain the weighted coefficient ratio probability in relation to extinction, scattering and absorption of light through a turbid medium. The next flux diagram in Fig. 1 shows the implementation of this algorithm in order to generate a program in Wolfram Mathematics.

The number of photons sensed by the photodetector is carried out thanks to the complex components from transverse plane of the step function. The Eqs. (5) and (6) are scalars that define the parallel and perpendicular components, respectively. Due to the complex nature of these equations, they can be viewed as phasors. Therefore, it is possible to associate orthogonal complex planes over plane XY (parallel components) and over plane YZ (perpendicular components), as is

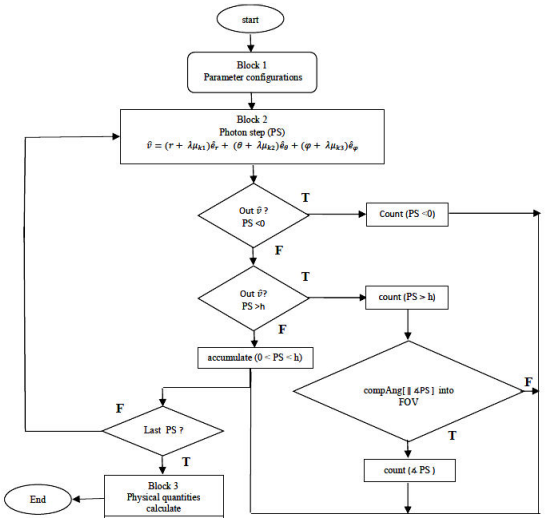

FIGURE 1. Flux diagram.

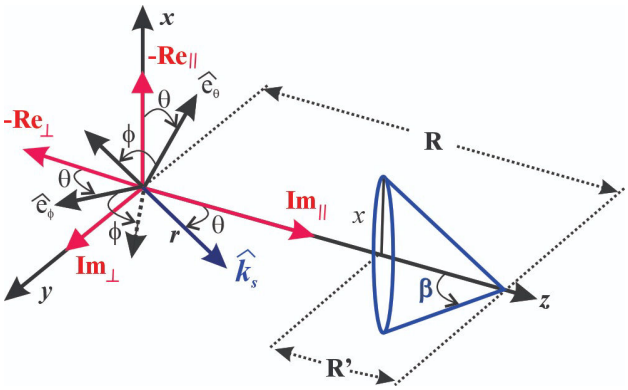

FIGURE 2. Superposition of parallel complex plane with perpendicular complex plane.

shown in Fig. 2. As a result, it is possible to obtain the photons path angular directions in relatively short machine times. The total numbers of photons sensed by the photodetector depended on the solid angle. The aperture angle is defined as [11]

$$\beta = \tan^{-1}\frac{x}{R'}. \tag{12}$$

3. Experimental process

Figure 3, shows the experimental setup assembled at the laboratory using an FPGA development card to generate a digital signal in PWM format whose frequency operation is 1 Hz. This digital signal is used to modulate a laser source whose central wavelength is 532 nm. The modulated light across a generated turbid medium enclosed in a transparent glass box of 10 cm of thickness. At the other end, a photodetector captures the light and its output is plugged in to an optical meter.

Turbid media (water cloud) is generated by putting hot and ice water in the bottom and upper of the glass box and match smoke is used as condensation nuclei. Figure 4 is a picture of the experimental setup indicating the components used.

Nine samples are obtained and registered at steps of 1 second. Subsequently, these data are used to adjust the MC-M model to confirm the average size of scatters and refraction index media proposed.

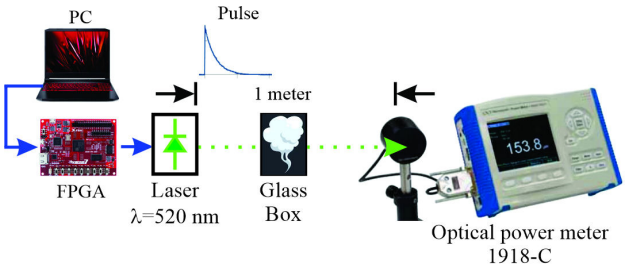

FIGURE 3. Experimental set up assembled.

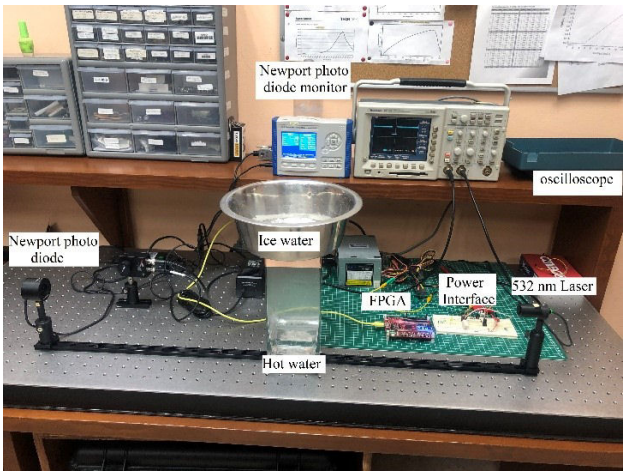

FIGURE 4. Experimental set up images.

4. Experimental parameters and specifications

Experimental parameters used in the experiment are: size of the particles compounded by turbid media, specifically water cloud scatterers, whose average radius is Rwc=10 μm [17]. Dimensions of the box, whose sizes are: 22 cm in height and 10 cm^2 in area. It is fabricated in conventional glass. Refracted index of dense glass and water cloud [18] besides other parameters of the turbid media, laser source and photodiode detector are, these values and specifications of the power detector are summarized in Table I.

In the process of capture of experimental data, a reference power level is measured through the glass box without water cloud.

TABLE I. Experimental parameters table.

Parameter	Symbol	Value (532 nm)
Cloud water, refracted index	m_{wv}	1.334
Crystal box, refracted Index	m_{gls}	1.66
Radius of glass particles	R_{gls}	100 nm
Radius of vapor water	R_{wc}	0.3-10 um
Condensation water vol	V_{ocw}	0.0022 m^3
Width of turbid media	Wd	0.1 m
Distance source-detrector	R	1 m
Optical power	Pt	-28.13 dBm
Spectral range	SR	400-1100 nm
Power (with attenuator)	Pwa	2w
Power (with-out attenuator)	Pwoa	4 mw
Pulse energy(W-attenuator)	EPwa	5 uJ
Pulse energy(Wo-attenuator)	EPwoa	5 uJ

TABLE II. Trapped, transmitted and backscattering average photons.

Radius	Trapped	Transmitted	Backscatt
3 um	$1.504 * 10^{-19}$	0.7552	0.2250
9 um	$1.523 * 10^{-19}$	0.940	0.0395
12 um	$5.249 * 10^{-19}$	0.9782	0.0020
27 um	$6.237 * 10^{-21}$	0.9795	0.00067

5. Simulation results

A series of 9 simulations are carried out considering a turbid medium, not absorbent. The simulation parameters are: an optical source whose central wavelength is 532 nm, an incident light pulse constituted by a population of 5×10^5 photons.100 scattering events, a thickness of a turbid medium of $h = 10$ cm, a refractive index of 1.334, radius dimension of scatterers $r = 3$ um , $r = 9$ um, $r = 12$ um and $r = 27$ um. Simulation results are summarized in Table II showing the trapped photons, transmitted photons, and backscattered photons at 532 nm of wavelength.

Also, the MC-M simulation counts the average probability photon sensed by a virtual photodetector considering 1 m of separation between the optical source. Figure 5 is an illustration of the mechanism of the impact of a photon and the sensed on the solid angle of the photodetector located at (R, 0, 0) distance [11].

Table III shows tabulates experimental and theoretical values data corresponding to the average probability photon sensed by FOV.

Figure 6 shows the graphic profile from the previously tabulated values.

As can be seen from this graph the Monte Carlo-Mie model works in a precise way for dense turbid media at the first three numerical events.

TABLE III. Experimental and Theoretical values.

Event	Experimental data	Theoretical data
1	0.3214	0.3173
2	0.2506	0.2620
3	0.3346	0.3293
4	0.5616	0.5913
5	0.6841	0.5917
6	0.7316	0.6466
7	0.7877	0.6470
8	0.7889	0.6589
9	0.7916	0.9086

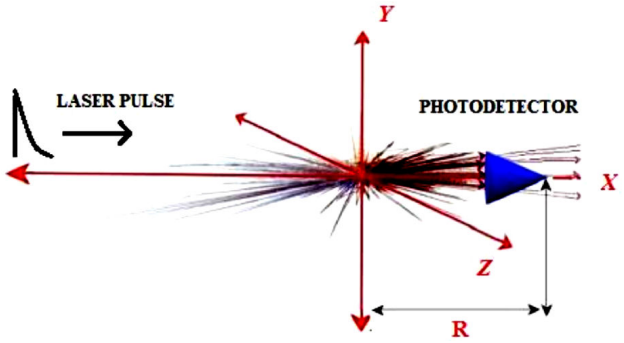

FIGURE 5. Average probability photons in forward scattering.

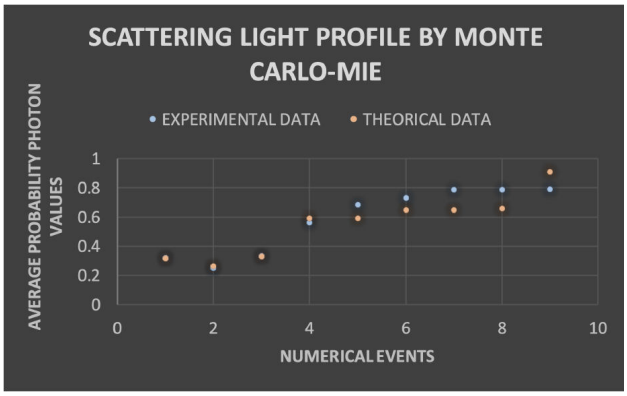

FIGURE 6. Experimental and theoretical values in the FOV.

6. Conclusion

The analysis of the scattering light using the Monte Carlo stochastic method approach, based on spherical harmonics, allowed us to obtain the average weighted rate of backscattering coefficient, scattering coefficient, and absorption coefficient through a turbid media, besides giving an approach to the average probability of photons sensed by the photodetector. Table II summarizes the Mie-phase function profiles of the populations of photons increasing the scattering of light in the forward direction, according to the size of the radius of the scatterer, specifically when the radius is increasing in size. The use of the MC-M algorithm provided for the first three experimental data values the minimum average error of 2.4 percent for the radius of 3, 9, and 12um of the scatterers; which corresponds to the case when the cloud is denser in the glass box. However, when the cloud was less dense, the rest of the 6 experimental values were not obtained with a minimum error. After a review of the data tabulated in Table III, it was possible to propose a different combination of radii. A superposition of two or three different sizes of 3,9,12 and 27um, was carried out to reduce the average error to near 13 percent. The authors conclude that this phenomenon is due to that when the temperature gradient is higher the average sizes of cloud drops are uniform. But, at a measure that this temperature gradient is lower, the average size is not uniform, and different average sizes could exist momentarily

until disappear. In summary, the Monte Carlo-Mie method works better for dense turbid than when it is not. Besides, this method allowed us to know some physical properties of the medium, as the average sizes of scattered particles and refracted index by using an investment model.

1. C. E. Wieners *et al*., Solar radiation modification is risky, but so is rejecting it: a call for balanced research, *Oxf. Open Clim. Chan*. **3** (2023) kgad002, https://doi.org/10.1093/oxfclm/kgad002.
2. L. Haoyu *et al*., A Monte Carlo method approach for the solution of the Helmholtz equation, In 2015 Asia-Pacific Microwave Conference (APMC), **vol. 3** (IEEE, 2015) pp. 1-3, https://doi.org/10.1109/APMC.2015.7413522.
3. W. Zhensen, Y. Yi, and C. Lihong, Monte Carlo simulation for millimeter wave propagation and scattering in rain medium, International *Int. J. Infrared Milli. Waves* **13** (1992) 981. https://doi.org/10.1007/BF01009622
4. L. R. Bissonnette *et al*., LIDAR multiple scattering from clouds, *Appl. Phys. B* **60** (1995) 355, https://doi.org/10.1007/BF01082271.
5. D. Toublanc, Henyey-Greenstein and Mie phase functions in Monte Carlo radiative transfer computations, *Applied optics* **35** (1996) 3270, https://doi.org/10.1364/AO.35.003270.
6. J. R. Mourant *et al*., Hemoglobin parameters from diffuse reflectance data, *J. Biomed. Opt.* **19** (2014) 037004, https://doi.org/10.1117/1.JBO.19.3.037004.
7. P. F. Liaparinos, Light wavelength effects in submicrometer phosphor materials using Mie scattering and Monte Carlo simulation, *Med. Phys.* **40** (2013) 101911, https://doi.org/10.1118/1.4821089.
8. Y. Ma *et al*., Multiple-scattering effects of atmosphere aerosols on light-transmission measurements, *Opt. Rev.* **24** (2017) 590, https://doi.org/10.1007/s10043-017-0352-9.
9. E. Torres-García *et al*., A new Monte Carlo code for light transport in biological tissue, *Medical and Biological Engineering and Computing* **56** (2018) 649, https://doi.org/10.1007/s11517-017-1713-z.
10. L. Pielsticker, R. Schlögl, and M. Greiner, Monte Carlo calculations for simulating electron scattering in gas phase, arXiv preprint arXiv:2101.01561 (2021), https://doi.org/10.48550/arXiv.2101.01561.
11. E. Pérez Mayesffer *et al*., 3D Monte Carlo analysis on photons step through turbid medium by Mie scattering, *Rev. Mex. Fis.* **67** (2021) 292, https://doi.org/10.31349/RevMexFis.67.292.
12. M. Subramanian, Atmospheric limitations for laser communications, (EASCON Record, 1968).
13. A. B. Magoun, David Sarnoff Research Center: RCA Labs to Sarnoff Corporation (Arcadia Publishing, 2003).
14. D. Aviv, Laser space communications (Artech Hause, 2006).
15. I. M. Sobol, Método de Montecarlo (Mir Moscu, 1983), pp. 32-47, 55-57.
16. C. F. Bohren and D. R. Huffman, Absorption and scattering of light by small particles (John Wiley & Sons, 2008), pp. 57-63, 82-103. https://doi.org/10.1002/9783527618156.
17. T. Y. Nakajima, K. Suzuki, and G. L. Stephens, Droplet growth in warm water clouds observed by the A-Train. Part I: Sensitivity analysis of the MODIS-derived cloud droplet sizes, *J. Atmos. Sci.* **67** (2010) 1884, https://doi.org/10.1175/2009JAS3280.1.
18. J. Rheims, J. Köser, and T. Wriedt, Refractive-index measurements in the near-IR using an Abbe refractometer, *Meas. Sci. Technol.* **8** (1997) 601, https://doi.org/10.1088/0957-0233/8/6/003.